Journal of Molecular Liquids 311 (2020) 113308

Contents lists available at ScienceDirect

Journal of Molecular Liquids

journal homepage: www.elsevier.com/locate/molliq

Ultrafast photophysical and nonlinear optical properties of novel free base and axially substituted phosphorus (V) corroles

Naga Krishnakanth Katturi [a], Shivaprasad Achary Balahoju [b], A.R. Ramya [b], Chinmoy Biswas [c], Sai Santosh Kumar Raavi [c], Lingamallu Giribabu [b,d,*], Venugopal Rao Soma [a,*]

[a] Advanced Research Centre for High Energy Materials (ACRHEM), University of Hyderabad, Hyderabad 500046, Telangana, India
[b] Polymers & Functional Materials Division, Tarnaka, CSIR-Indian Institute of Chemical Technology, Hyderabad 500007, Telangana, India
[c] Ultrafast Photophysics and Photonics Laboratory, Department of Physics, Indian Institute of Technology Hyderabad, Kandi 502285, Telangana, India
[d] Academy of Scientific and Innovative Research (AcSIR), AnusandhanBhawan, 2 Rafi Marg, New Delhi, 110001, India

ARTICLE INFO

Article history:
Received 24 December 2019
Received in revised form 1 May 2020
Accepted 5 May 2020
Available online 8 May 2020

Keywords:
Corroles
Transient absorption
Z-scan
Excited-state dynamics
Two-photon absorption

ABSTRACT

The progression in synthetic procedures over the last two decades gave admittance to a wide variety of corroles for suitable potential applications such as photovoltaics, photonics, and bio-imaging. In this communication, we present results from our investigations of ultrafast photophysical processes and third-order nonlinear optical properties of newly synthesized donor-acceptor based free-base [$(C_6F_5)_3$] and phosphorus [P-$(OH)_2(C_6F_5)_3$] corroles. The global analysis of the femtosecond transient absorption data based on the compartmental model revealed the corresponding time constants of several photophysical processes such as (a) internal conversion (τ_{IC}) in the 260–280 fs range (b) vibrational relaxation (τ_{VR}) in the 2.5-5 ps range and (c) nonradiative relaxation times (τ_{nr}) in the 4.15–7.6 ns range and finally (d) triplet lifetimes in the range of 25–50 μs. The two-photon absorption (TPA) cross-section measurements were performed using the femtosecond, kHz pulse *Z*-Scan technique at 600 nm and 800 nm and the retrieved TPA cross-section values were in the range of ~10^2 GM. Degenerate four-wave mixing measurements illustrated a large third-order nonlinear optical susceptibility $\chi^{(3)}$ with a magnitude of 6.9×10^{-14} esu and instantaneous (sub-picosecond) response, suggesting a pure electronic contribution to the nonlinearity of these corroles. The discoveries from this study may help further to extend the capability of corroles as NLO materials for photonic applications.

1. Introduction

Unique, organic molecules possessing stable and strong optical/nonlinear optical (NLO) properties are a prerequisite for diverse applications in photonics, bio-imaging, photovoltaic, and photocatalysis [1–3]. Notably, organic molecules possessing large π-conjugation, specially corroles with donor-acceptor (D-A) systems, are suitable for many applications, mainly photovoltaics [4–8] and up-conversion [9] due to close structural similarities of natural photosynthetic pigments [10–12]. They also exhibit strong NLO properties arising from its larger π-electron conjugation [13–18]. Organic moieties holding π-bond conjugation are known to illustrate stronger dipole moments and create a delocalized distribution of electric charges due to intramolecular charge transfer (ICT) resulting in high electrical polarization, which is advantageous for large NLO response [19–24]. A few reports on natural photosynthetic phenomena of D-A systems based corroles can be found from the literature [25–29]. Such D-A systems have been designed by altering the local position of metal ion of the corrole macrocycle, for example, either at the axial or at the *meso*-phenyl position.

In the tetrapyrrolic family, corroles are new chromophores similar to porphyrinoids possessing 18 π–electron aromaticity identical to that of porphyrins. Corrole ring consists of four nitrogen atoms in the core and 19 carbons atoms in the molecule. When compared to porphyrins, corroles are having attractive properties such as stability, higher fluorescence, intense absorption in the red region of the optical band, lower oxidation potentials, and more significant stoke shifts. In corroles, the three central nitrogen atoms can stabilize the higher oxidation states of different metals, which make the corroles a suitable material for many different fields, in artificial photosynthesis and biomedical applications [9,30]. By attaching the various metals and transition metals to the corrole macrocycle, one can tune the optical properties due to change in the energy gap of the molecular orbitals, which can be used for biomedical imaging and sensing [31–35]. Efficient photo-induced electron transfer (PET) and triplet photosensitization can be achieved by donor-acceptor based molecular systems with long relaxation

* Corresponding authors.
E-mail addresses: giribabu@iict.res.in (L. Giribabu), soma_venu@uohyd.ac.in, svrsp@uohyd.ernet.in (V.R. Soma).

https://doi.org/10.1016/j.molliq.2020.113308
0167-7322/

times [4,36–38]. PET is the fundamental process in photosynthesis and different artificial photo-devices. The triplet photosensitizers should have efficient intersystem crossing to achieve triplet excited states. This is possible by adding the metal/transition metal to the corrole macrocycle provided high fluorescence quantum yields [9,39–43]. Liu et al. [44] have performed a comparative study of the excited state dynamics of Al and Ga corroles wherein they found that corroles are planar rigid frameworks with large Frank-Condon vibration states possessing large S_2 displacements compared to metalloporphyrins. They recorded lifetimes of the S_2 states to be 520 fs and 280 fs in Al(tpfc)(py) corrole and Ga(tpfc)(py) corrole, respectively. Raavi et al. [45] recently presented a systematic photophysical investigation on a series of Phosphorous (P-TTC) and Germanium (Ge-TTC) based corroles dissolved in toluene occurring in the femtosecond to microsecond time scales and concluded that Ge-TTC had superior triplet state properties compared to P-TTC. Therefore, understanding these ultrafast photophysical processes, especially in newly designed and developed molecules, is essential for the development of new systems, enabling them to find potential applications.

On the other side, the NLO properties of corroles have evoked tremendous interest due to their highly conjugated π-electron distribution compared to porphyrins. Several authors have investigated the NLO behavior of different corroles, and they found significant NLO coefficients [16,46] when compared to porphyrins. Although the NLO properties of corroles are superior to porphyrins, very few reports are found in NLO activity. In general, for an efficient NLO activity, the material should consist of high refractive index n_2 values with an instantaneous response. In this work, we have synthesized a novel free-base and axially substituted phosphorus corroles. The investigation of their photophysical process and third-order NLO properties and response were studied in the solution phase. The transient absorption studies show the long triplet decay times in the case of phosphorus corrole and strongly excited state absorption behavior. We observed significantly strong NLO coefficients and TPA cross-section (~190 GM) along with Kerr-type nonlinear refractive index ($n_2 \sim 10^{-15}$ cm^2/W) from the synthesized corroles.

2. Experimental details

2.1. Synthesis

Synthesis of 5,10,15-tris(pentafluorophenyl)corrole (C_6F_5-Corrole) and phosphorous complex of C_6F_5-Corrole (P-$(OH)_2(C_6F_5)_3$-Corrole) have been reported in literature [47,48]. The steady-state UV absorption and emission spectra were obtained by using the PerkinElmer spectrophotometer and Fluorolog (M/s HORIBA). The samples were dissolved in a pure DMF to prepare the diluted solutions of ~25 μM concentration. The prepared samples are filled in a 1-cm quartz cuvette and kept sealed for all the measurements. The measurements were performed at room temperature. The fluorescence spectra are recorded at 410 nm excitation, and the spectra were obtained in the 300–750 nm spectral range.

2.2. Transient absorption measurements

Transient absorption (TA) measurements were performed by using a commercial HELIOS spectrometer based on a femtosecond (fs) laser system. The complete experimental details can found from our previous work [49]. Laser pulses from a femtosecond amplifier (LIBRA, M/s Coherent, USA) generating ~50 fs pulses at 1 kHz, 800 nm wavelength were used to pump the TA spectrometer. The output from the amplifier pulses 800 nm was divided into two parts. One part of the laser was focused onto a 2-mm thick sapphire plate to obtain a probe light spectrum from 430 nm to 800 nm, and the probe light was collimated using a set of parabolic mirrors to overcome the group velocity dispersion effects. The probe pulse was placed on a linear stage (Thorlabs) before the sample to achieve the time delay between pump and probe pulses. The other part of the laser was allowed to pass through a BBO (beta barium borate) NLO crystal to generate the second harmonic at 400 nm, which was used as the pump beam. The pump beam was chopped at 500 Hz to enhance the signal to noise ratio. The sample (in a 1-mm cuvette, at ~25 μM concentration in DMF solvent) was placed on an XY-translating stage to minimize the sample degradation effects. The energy of pump pulses was kept at 0.15 μJ. The transmitted probe pulse was collected by using a spectrometer (ocean optics). The complete measurements were performed at room temperature. The TA spectra are globally analyzed by using Glotaran software (based on TIMP R-package) [50,51].

2.3. Transient absorption data analysis

To achieve a precise decay rate constants and spectra of excited-state species, the TA spectra is globally analyzed using a compartmental model [52]. The global analysis provides a detailed explanation of the TA data at all measured wavelengths and time points simultaneously. This was performed by fitting the TA spectra with number of independent exponential components. The number of independent components can be estimated by singular value decomposition (SVD) method. First, the TA spectra are fitted to a sequential model consisting of evolution associated difference spectra (EADS), which provide the information about the evolution of excited-state species. The sequential model provides an estimation of respective time decay constants, which can be used for further investigation of the system based on target analysis using the compartmental model. In general, EADS contains a mixture of contributions from different processes. To extract the information from pure excited state and product states, a specific model can be attributed so-called target analysis, which provides the individual species associated difference spectra (SADS). From this model, the energy and charge transfer processes can be estimated in terms of different reaction mechanisms or different compartments.

2.4. Z-scan measurements

The third-order NLO properties were measured using a single beam Z-scan technique. An optical parametric amplifier (OPA, TOPAS-C) is used as a laser source which is pumped by a 50 fs 800 nm laser amplifier (LIBRA).The input laser pulses from OPA (at 600 nm and 800 nm) were focused on using a 15 cm lens, and the sample is translated along the Z direction by using a linear translation stage (Newport). The input beam diameter is ~3 mm with a beam waist (ω_0) of 50 μm and the corresponding Rayleigh range being ~2.0 mm. The input intensities are calculated to be in the range of ~60–110 GW/cm^2. The transmitted signal was collected using a photodiode (PD, Thorlabs SM1PD2A). The PD is connected to a lock-in amplifier (Signal recovery 7265). The voltage output from the lock-in amplifier was recorded at each sample position. A 1-mm sample cuvette was used to hold the sample and the acquisition was performed through a LabVIEW program. The complete experimental details can be found in our previous work [53].

2.5. Degenerate four-wave mixing measurements

Degenerate four-wave mixing experiments were performed using ~50 fs pulses. The output of the amplifier pulses was divided into three equal parts and arranged in a forward BOXCAR geometry fashion. The energy of all the three input beams were nearly the same (~1.2 μJ). A 5-mm sample cuvette was used for the measurements to hold the sample (0.1 mM concentration in DMF solvent). The signal which appeared as the fourth beam and was obtained at the fourth corner of the BOX was fed to a lock-in amplifier (signal recovery 7265) by using a photodiode (Thorlabs SM1PDA). The complete experimental details can be found in our previous work [53]. The time-resolved DFWM transients were recorded at each probe delay using a LabVIEW program.

3. Results and discussions

3.1. Steady-state absorption and emission spectra

The steady-state absorption spectra of two corroles $(C_6F_5)_3$-Corrole and P-$(OH)_2(C_6F_5)_3$-Corrole are shown in Fig. 1(a) and (b) (black curves). An intense peak [Soret band (S_2)] near 430 nm for the free-base corrole was observed, which arises mainly due to π-π* electronic transitions from the ground state to the second excited state (S_2). The Soret band of phosphorus corrole with a blue shift at 410 nm was observed. The inset displays the magnified view of the Q-band absorption due to the π-π* transition from the ground state to the first excited state (S_1). The steady-state emission spectra of the synthesized corroles were recorded at 410 nm excitation, as shown in Fig. 1(a) and 1(b) (red curves). The photophysical parameters and DFT studies were reported in our earlier work [54], with the corresponding molecular structure are shown in Fig. 1(c) and (d). The energies of HOMO-LUMO were 5.80 eV, and 2.88 eV and 5.32 eV and 2.79 eV for phosphorus(V) corrole and C_6F_5-corrole respectively [54,55], and the fluorescence quantum yields are found to be $\Phi = 0.53$ and $\Phi = 0.14$ in phosphorus(V) corrole and C_6F_5-corrole with singlet excited state lifetime of 3.6 ns and 3.7 ns in solution state (dichloromethane) [29,54].

3.2. Transient absorption measurements

The femtosecond transient absorption (TA) measurements were performed at Soret band photoexcitation with 400 nm wavelength. The TA spectra were measured up to 3 ns delay from 450 to 780 nm wavelength range. Fig. 2(a)-(b) depict the transient absorption spectra of the C_6F_5-Corrole and P-$(OH)_2(C_6F_5)_3$-Corrole recordedin DMF solvent. The phosphorus corrole exhibited a strong photobleach signal at 590 nm compared to free-base corrole indicating with slow recovery due to the possible formation of long-lived photo-excited species perhaps resulting from a higher triplet yield. The TA spectra illustrated three different absorption peaks upon photoexcitation I) photo-induced absorption band in the spectral range 450–550 nm due to excited state absorption including the formation of triplet-triplet state absorption II) a negative signal in the spectral range of 556–615 nm due to S_0 ground state bleach (GSB) with Q-band vibrational features and III) stimulated emission peak near 647 nm for phosphorus corrole and 685 nm for free base corrole. A closer look into the TA spectra of phosphorus corrole up to 10 ps, shown in Fig. 2(c)-(d), reveals various processes: (i) After the photoexcitation with 400 nm positive bands at 465 nm and 714 nm and negative bands at 590 nm and 566 nm are instantaneously formed, and the positive groups are assigned to singlet excited state absorption whereas the negative signals to ground state bleach, (ii) The bleach maximum at 590 nm of phosphorus corrole increases up to 50 ps, and the Q vibrational band at 570 nm stays up to 1 ps time scale, and (iii) the stimulated emission peak near 645 nm, that continues to increase up to 100 ps and after that starts decaying which is due to the relaxation of singlet relaxed excited state (Fig. 2 (a)-(b)).

In the case of free base corrole, the SE band near 685 nm decays within 1 ns, and the bleach maximum at 620 nm increases up to 10 ps. At a 10 ps time scale, a blue shift in the spectra shown in Fig. 2 (c)-(d) is evident from both the spectra; after that, it starts decaying continuously. This represents the two different species spectra before and after a 10 ps time scale, which could be due to the vibrational relaxation to the S_1 excited state at that time scale. The longer decay of the bleach signal due to the loss of excited state absorption confirms the formation of triplet states, as seen in Fig. 2(a), (b). Understanding the ultrafast photophysical process by single wavelength analysis is difficult due to the overlapping of different photo processes. Therefore, global analysis based on target model was performed on both the spectra free-base and phosphorus corrole to get a complete picture of the various photo process involved such as I) internal conversion (from the lowest vibrational states of S_n to the highest vibrational states of S_1) II) vibrational relaxation (within the S_1 state) III) nonradiative relaxation [including

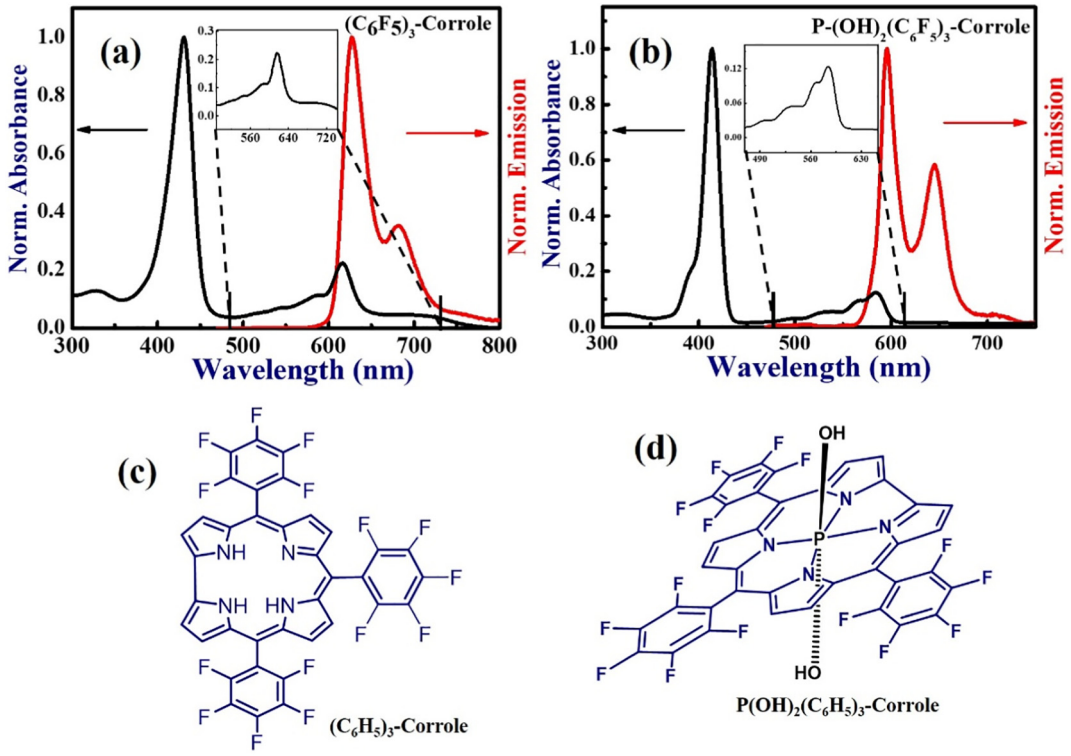

Fig. 1. Absorption and emission spectra of (a) $(C_6H_5)_3$-Corrole and (b) P-$(OH)_2(C_6F_5)_3$-Corrole in DMF solvent (c) and (d) Molecular structure of the title molecules investigated in the present study.

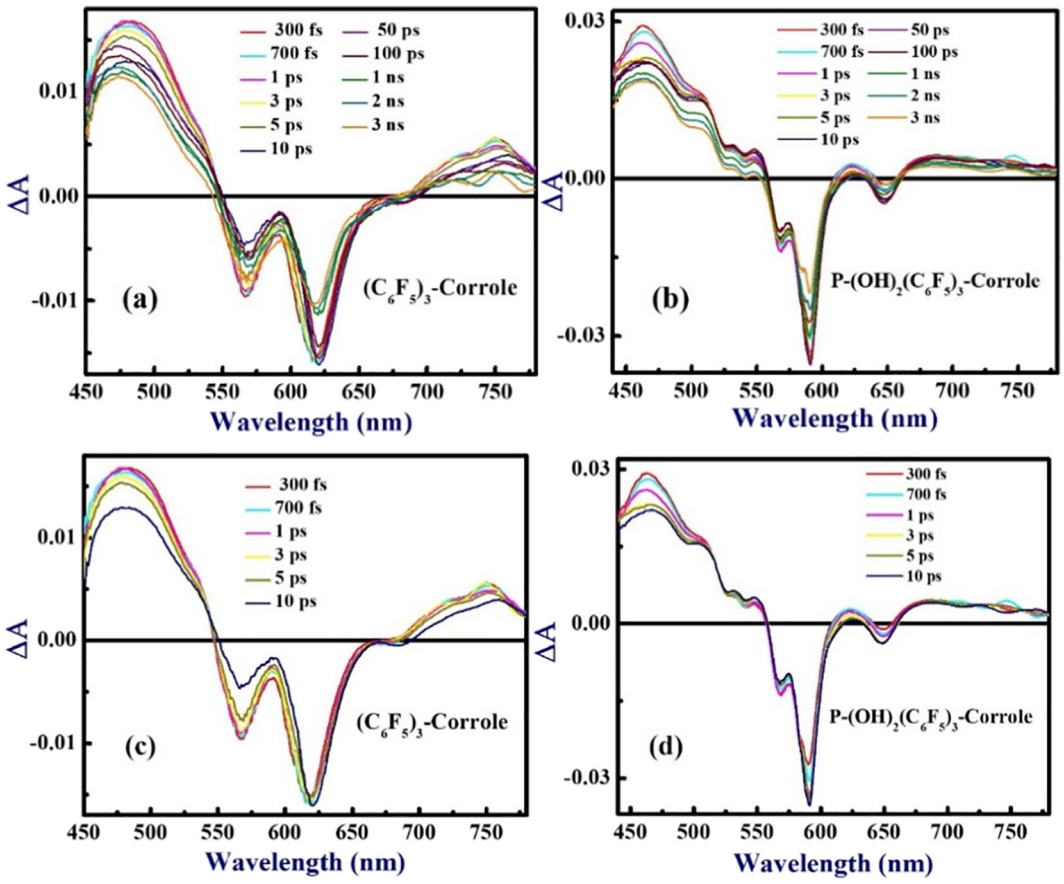

Fig. 2. fs-TA spectra of (a) $(C_6F_5)_3$-Corrole and (b) P-$(OH)_2(C_6F_5)_3$-Corroleat different probe delays and TA spectra of (c) $(C_6F_5)_3$-Corrole and (d) P-$(OH)_2(C_6F_5)_3$-Corrole at a shorter time scale up to 10 ps.

the intersystem crossing (S_1 states to T_1 states) and nonradiative relaxation directly from S_1 states to S_0 states and IV) triplet decay (T_0-S_0) wherein the population from T_0 states relaxes to ground state S_0.

Fig. 3 shows the TA kinetic profiles along with fittings at selected wavelengths for phosphorus corrole and free-base corrole obtained after the target analysis. The displayed wavelengths represent different photo process after photoexcitation at 400 nm. The kinetics of phosphorus corrole at Q-band at 590 nm (GSB) did not decay even after 3 ns, which suggests the formation of long-lived excited species. The kinetics of the SE band maxima at 648 nm is decayed within ~2 ns in the case of phosphorus corrole, whereas in the case of free-base corrole kinetics of the SE band at 683 nm completely decays within 1 ns suggesting the formation of triplet states at this time scales. A kinetic analysis based on a compartmental scheme was implemented by using a photophysical model, as shown in Fig. 4, which helps to estimate the spectra of excited species providing corresponding species associated difference spectra (SADS) and microscopic rate constants of individual species shown in Fig. 5.

Fig. 5 shows the target analysis for the phosphorus corrole and free-base corrole TA spectra with respective SADS (left) and population (right) decay profiles. From the target analysis of the phosphorus corrole TA spectra based on the photophysical model (Fig. 4), we

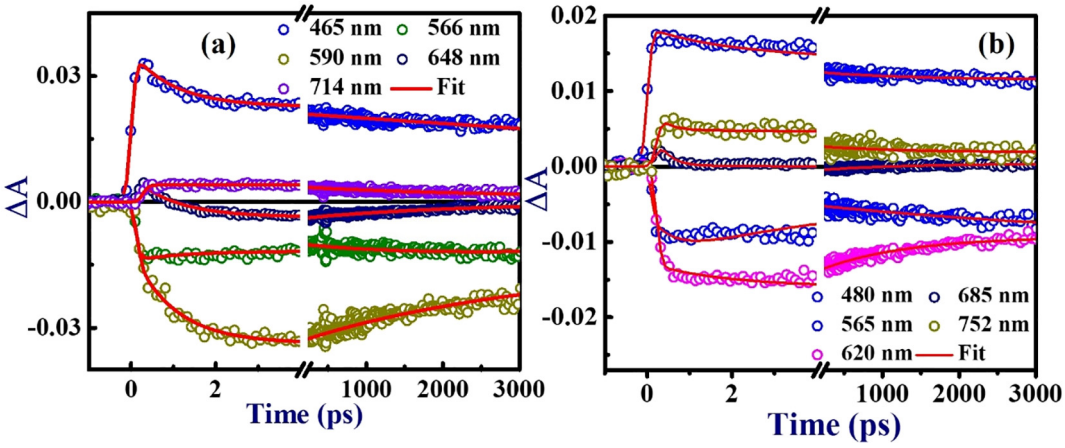

Fig. 3. TA kinetics of (a) $(C_6F_5)_3$-Corrole and (b) P-$(OH)_2(C_6F_5)_3$-Corroleat selected wavelengths scattered points are experiential data while the solid lines are theoretical fits.

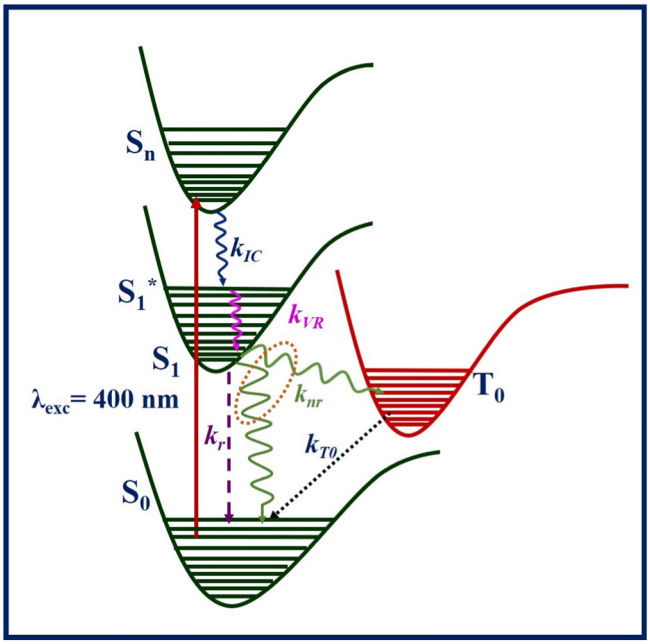

Fig. 4. Schematic of the representative energy band model taken for global analysis.

estimated the internal conversion (IC) rate (S_n to S_1^* states) as $k_{IC} = 3.8 \times 10^{12}\ s^{-1}$ corresponding to a lifetime of 260 fs, vibrational relaxation (VR) rate (from S_1^* to S_1 states) constant as $k_{VR} = 4 \times 10^{11}\ s^{-1}$ corresponding to a lifetime of 2.5 ps and triplet relaxation from T_0 to S_0 with life time estimated to be 25 μs. The lifetime of S_1 state was fixed using the value obtained from the TCSPC measurements, which was 3.6 ns. We used $\tau_{TCSPC} = [1 / (k_r + k_{nr})]$ wherein 'τ_{TCSPC}' is the lifetime obtained from measurements and k_r being the radiative decay rate and k_{nr} being the nonradiative decay rate (the population from S_1 state can come down to the ground state of S_0 directly or through T_0 (via ISC) [29,54]. From S_1 state 53% of population goes radiatively to the ground state with 6.7 ns lifetime (obtained from fluorescence quantum yield) and the remaining 47% is transferred to non-radiatively with a 7.6 ns lifetime constant. In case of free-base corrole the life time of S_1 state was obtained as 3.7 ns, where 14% population from S_1 state goes radiatively to S_0 with lifetime of 25.5 ns and 86% of population is transferred nonradiatively to ground state with lifetime of 4.15 ns. We have obtained an excellent agreement between the theoretical fits and the experimental TA data. Fig. 6 demonstrates the significant overlap of TA data (scattered points) and theoretical fit (solid lines) at 0.3 ps and 3 ns probe delay times of the synthesized corroles. Table 1 summarizes the estimated photophysical parameters from the target analysis. The errors in the lifetimes estimated were estimated to be <1%.

Fig. 5(a) and (c) illustrate the SADS spectra of two corroles and individual population decay profiles Fig. 5(b) and (c) of different excited state processes after photoexcitation with 400 nm. The SADS spectra of Corroles brings the distinction between different processes, the SADS1 (left) corresponds to the formation of higher excited state S_n and SADS 2, and 3 represents the vibrational hot S_1^*states and relaxed S_1 state. The SADS4 could be due to the relaxation of the triplet state.

3.3. Nonlinear optical properties

3.3.1. Z-scan

The third-order NLO properties of synthesized Corrole were investigated at 600 nm and 800 nm wavelength by using a 50 fs laser pulses using a Z-scan technique with an input intensity of ~50 GW/cm^2. All the measurements were performed in a solution phase at room temperature with solution processing concentration ~ 0.1 mM in pure DMF.

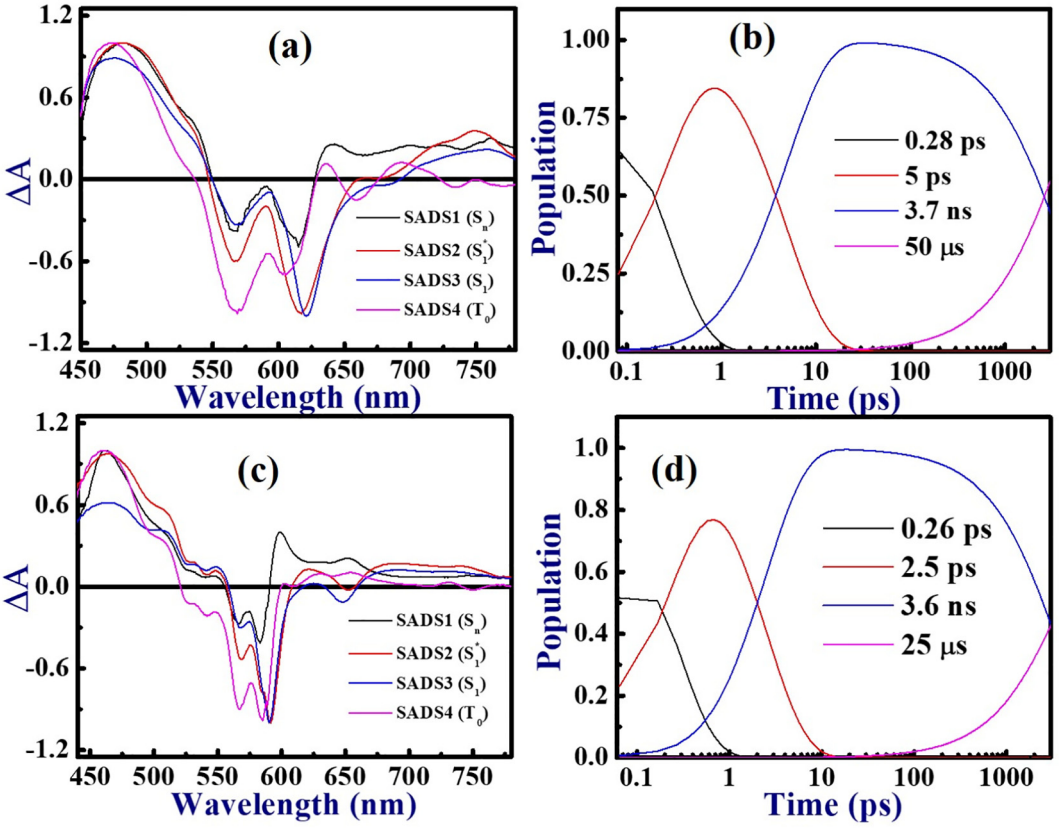

Fig. 5. SADS (left) and concentration profiles (right) of (a, c) $(C_6F_5)_3$-Corrole and (b, d) P-$(OH)_2(C_6F_5)_3$-Corrole.

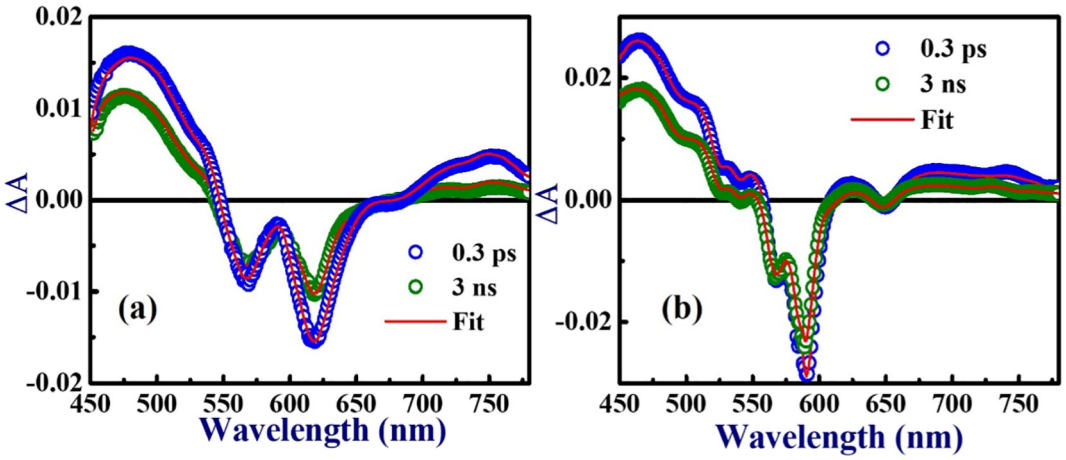

Fig. 6. fs-TA spectra of (a) $(C_6F_5)_3$-Corrole and (b) P-$(OH)_2(C_6F_5)_3$-Corroleat a pump−probe delay of 0.3 ps and 3 ns depicting an excellent agreement of the global fitting (solid line) with the experimental data (circles).

From the obtained Z-scan transmission curves, two-photon absorption coefficient (β) and nonlinear refractive index (n_2) and corresponding third-order nonlinear susceptibility $\chi^{(3)}$ were extracted. The open aperture (OA) transmission curves show the reverse saturable absorption behavior, as shown in the data presented in Figs. 7 and 8. The OA transmission curves were fitted using a standard two-photon absorption Eq. (1),

$$T_{OA(nPA)} = \frac{1}{\left[1+(n-1)\alpha_n L\left(I_0/\left(1+(z/z_0)^2\right)\right)^{n-1}\right]^{1/n-1}} \quad (1)$$

$$T_{CA} = 1 \pm \frac{4\Delta\Phi\left(\frac{z}{z_0}\right)}{\left[\left(\frac{z}{z_0}\right)^2+9\right]\left[\left(\frac{z}{z_0}\right)^2+1\right]} \quad (2)$$

where L is the effective path length of the sample $L_{eff} = \frac{1-e^{-\alpha_0 L}}{\alpha_0}$, Z_0 is the Rayleigh range $Z_0 = \frac{\pi\omega_0^2}{\lambda}$, ω_0 is the beam waist at focus (Z = 0), I_0 is the peak intensity.

The two-photon absorption cross-sections were obtained from $\sigma_n = \frac{(\hbar\omega)^{n-1}}{N}\alpha_n$ $(n = 2)$ where ω is input laser frequency, and N is the concentration of the sample. The obtained NLO coefficients are listed in Table 2. The errors in the NLO coefficients are estimated to be <5% arising predominantly from input peak intensity estimation. Phosphorus corrole exhibited a strong two-photon absorption coefficient (4.6×10^{-13} cm/W) compared to free-base corrole, possibly due to the effect of phosphorous ion [16,54,56]. The two-photon absorption cross-section values are found to be stronger compared to recently reported molecules [16,17,46,56–58]. Figs. 7 (b)-(d) and 8 (b)-(d) illustrate the closed aperture Z-scan curves, and the valley followed by a peak suggests positive type nonlinear refractive index (n_2) and self-focusing behavior with the magnitude of ~10^{-15} cm^2/W. We measured the nonlinearity of the solvent and found that the solute+solvent nonlinearity was higher than that of solvent alone. It is pertinent to mention here that the n_2 measured was for the solutions prepared with typical 100 μM concentrations. One needs to prepare thin solid films using these molecules or doped them into glasses to ascertain the actual magnitude of the solute nonlinearity. Further, there is a finite probability of laser pulses heating up the solvent, thereby resulting in thermal contribution to the overall nonlinearity. However, since the pulse duration is extremely short and the input pulse energies are too low, we believe that the thermal contribution in this case could be minimal and may require further experiments to quantify that. Those studies will be taken up in future.

The two-photon absorption in D-A systems is accompanied by a charge transfer process between donor and acceptor molecules such as metal and transition metals ions [58]. Rao et al. [13] recently reported that TPA coefficients from tritolylcorrole (TTC) and triphenylcorrole (TPC) were in the range of 10^{-13} cm/W, using ~ 40 f. laser pulses at 800 nm. Further, Anusha et al. [56] reported the TPA coefficient from germanium-substituted TTC (GeTTC) and phosphorus substituted TTC (PTTC) corroles with a magnitude of ~10^{-12} cm/W using ~ 2 ps laser pulses again at an input wavelength of 800 nm. Garai et al. [17] have investigated the NLO properties of trans-A2B-corroles, and they reported values of TPA (β) coefficients and nonlinear refractive index (n_2) values of 10^{-13} cm/W and ~ 10^{-14} cm^2/W obtained using 250 f. pulses at 80 MHz at 1064 nm. Recently, Yadav et al. [46]. studied the NLO activity of push-pull trans-A2B corroles with ~150 f. pulses but at MHz repetition rate (femtosecond oscillator pulses). They found strong nonlinear coefficients by two-electron withdrawing groups at *meso* position. Rebane et al. [16] showed TPA cross-section values of 60–130 GM (~70 fs,1 kHz repetition rate laser pulses) in *meso*-substituted A3 corroles, and they found that the cross-section values depended on

Table 1
Estimated photophysical parameters of the corroles investigated obtained from the global analysis. The values in the parenthesis indicate the relevant lifetimes.

Sample	k_{IC} 10^{12} s^{-1} (τ_{IC})	k_{VR} 10^{12} s^{-1} (τ_{VR})	k_r 10^9 s^{-1} (τ_r)	k_{nr} 10^9 s^{-1} (τ_{nr})	k_{T0} 10^4 s^{-1} (τ_{T0})
C_6F_5-Corrole	3.5 (280 fs)	0.2 (5.0 ps)	0.0392 (25.5 ns)	0.2622 (4.15 ns)	2 50 μs
P-$(OH)_2(C_6F_5)_3$-Corrole	3.8 (260 fs)	0.4 (2.5 ps)	0.1484 (6.7 ns)	0.1316 (7.6 ns)	4 25 μs

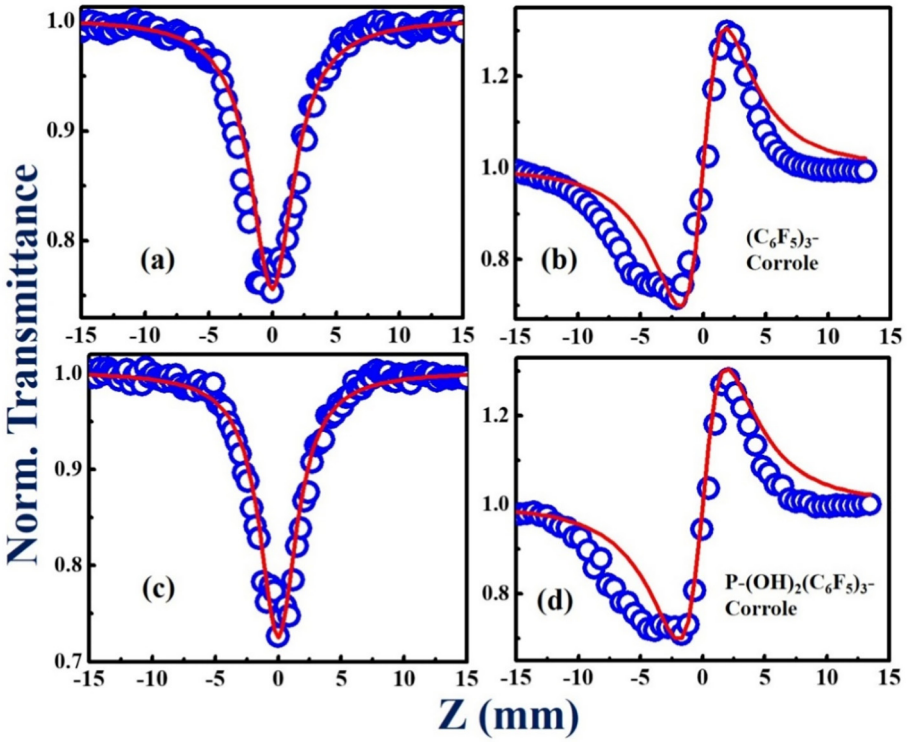

Fig. 7. (a)-(c) Open aperture *Z*-scan data (d)-(d) closed aperture Z-scan data of $(C_6F_5)_3$-Corrole and P-$(OH)_2(C_6F_5)_3$-Corrole, respectively, recorded at 600 nm with 50 fs, 1 kHz pulses and for 25 μM concentration solutions.

electron accepting capability of the substituents. The axially substituted phosphorus corrole has stronger NLO activity compared to free-base corrole possibly due to minimization of aggregation. Organic molecules-based donor-acceptor systems can have significant dipole moments by altering the donor or acceptor ions providing strong π-conjugation, and may produces intense electronic polarization. The enhancement of the obtained NLO coefficients from the phosphorus(V) corrole could be attributed to its strong electron withdrawing nature from the pentafluorophenyl group and possibly a strong intramolecular charge transfer between phosphorus and pentafluorophenyl group

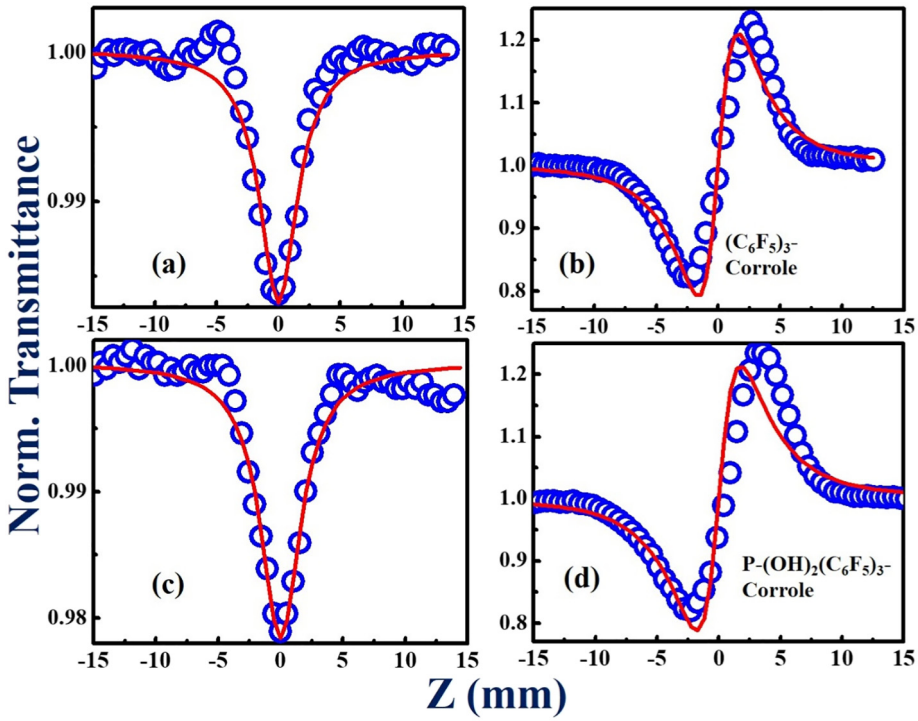

Fig. 8. (a)-(c) Open aperture Z-scan data (b)-(d) closed aperture Z-scan data of $(C_6F_5)_3$-Corrole and P-$(OH)_2(C_6F_5)_3$-Corrole, respectively, recorded at 800 nm with 50 fs, 1 kHz pulses. and for 25 μM concentration solutions.

Table 2
Summary of the NLO coefficients of corroles obtained using the *Z*-scan technique at 800 nm.

Sample	λ	α_2 cm/W $\times10^{-13}$	$\sigma_{(TPA)}$ GM	n_2 cm^2/W $\times10^{-15}$	$\chi^{(R)}$ m^2/v^2 $\times10^{-21}$	$\chi^{(I)}$ m^2/v^2 $\times10^{-24}$	$\chi^{(3)}$ m^2/v^2 $\times10^{-21}$	$\chi^{(3)}$ esu $\times10^{-13}$
P-$(OH)_2(C_6F_5)_3$-Corrole	800 nm	4.6	190	2.3	2.5	3.2	2.50	1.80
C_6F_5-Corrole		3.2	130	1.4	1.5	2.2	1.50	1.10
P-$(OH)_2(C_6F_5)_3$-Corrole	600 nm	4.4	181	2.0	2.15	2.3	2.14	1.54
C_6F_5-Corrole		2.5	103	2.1	2.25	1.3	2.24	1.61

which creates the large dipole moments. The TPA coefficients and corresponding TPA cross-section values suggest that the synthesized corroles can find applications in two-photon absorption-based bio-imaging, photonics, and optical switching devices.

3.4. DFWM data analysis

The DFWM experiments were carried at 800 nm wavelength in a forward BOXCAR-geometry. Figs. 9(a)-(c) illustrate the cubic dependency of the DFWM signal on the input energy, confirming the third-order NLO process measured in the solution phase at ~0.1 mM concentration achieved from DMF indicates the nonlinearity acts as Kerr-like fashion (with a slope of ~3.04). DFWM is an efficient technique to obtain the $\chi^{(3)}$ since the effect of linear scattering does not contribute to the signal, as in the case of the *Z*-scan technique. DFWM provides the time response of the optical nonlinearity. Z-scan measurements have contributions occasionally from linear scattering, sample imperfections, and laser beam shape. Thus, DFWM experiment is a better choice to measure the accurate magnitude of third-order nonlinearity when the sample possesses scattering or other issues. A pure solvent [Carbontetrachloride (CCl_4)] was utilized as a reference with $\chi^{(3)} = 4.4 \times 10^{-14}$ esu and the third-order nonlinear susceptibility $\chi^{(3)}$ was calculated using the standard procedure [53]. We have noticed a slightly higher value of $\chi^{(3)}$ in phosphorus corrole compared to the free-base corrole. The $\chi^{(3)}$ values were 6.2×10^{-14} esu and 6.9×10^{-14} esu for $(C_6F_5)_3$-Corrole and P-$(OH)_2(C_6F_5)_3$-Corrole, respectively. A $\chi^{(3)}$of 4×10^{-14} esu was obtained from the pure solvent (DMF) measured at the same experimental conditions. The $\chi^{(3)}$ values obtained in the DFWM and *Z*-scan experiments vary slightly (by a factor of 2–2.5) and this could be attributed to the stringent alignment in DFWM experiments wherein we possibly have underestimated the value and have slightly overestimated the values in the Z-scan experiments owing to errors in the peak intensity measurements.

The time-resolved DFWM signal was recorded as a function of probe delay and the signal was found to be nearly symmetric about the origin (zero delay). The TR-DFWM signal was fitted to a Gaussian function. The full-width half maxima (FWHM) of ~110 fs confirmed the instantaneous response, which suggests the pure electronic contribution (Kerr effect) to the nonlinearity as shown in the data of Figs. 9(d)-(f). The obtained $\chi^{(3)}$ values are similar or higher in magnitude than some of the reported works on metal-based organic moieties such as metallophthalocyanines and porphyrins [59,60]. The fast response and strong magnitude of $\chi^{(3)}$ suggest these molecules can find applications in all-optical switching and optical limiting.

4. Conclusions

In the present work, a detailed photophysical investigation and the ultrafast NLO studies of axially substituted phosphorus P-$(OH)_2(C_6F_5)_3$-Corroleand free-base $(C_6F_5)_3$-Corrole, has been performed. Femtosecond

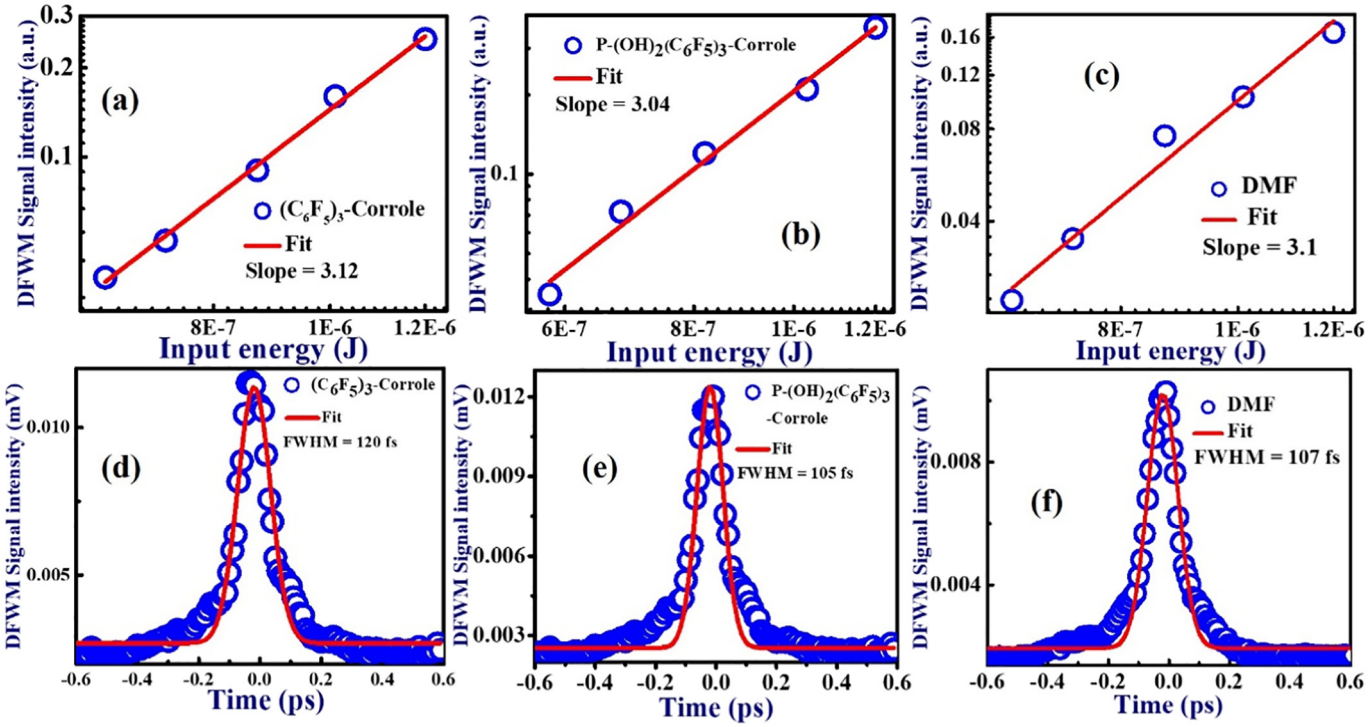

Fig. 9. Cubic dependency of the DFWM signal on input energy and time-resolved DFWM signal profiles of (a, d) $(C_6F_5)_3$-Corrole, (b, e) P-$(OH)_2(C_6F_5)_3$-Corrole and (e, f) DMF solvent.The solid line is theoretical fits, and scattered points are experimental data.

transient absorption spectroscopic measurements elucidated the evolution of various photophysical processes. With the specific target analysis of the TA spectra, we estimated rate constants for IC, VR, nonradiative, and triplet relaxation. From the TAS data analysis we observed that phosphorus corrole exhibited strong excited and triplet state properties compared to free-base corrole. The third-order NLO properties of synthesized corroles were explored using *Z*-scan and DFWM experiments with femtosecond, kHz pulses. The obtained NLO coefficients were found to be stronger in both the corroles compared to some of the recently reported corroles. The two-photon absorption cross-sections were found to be considerably large (30–190 GM) compared to some of the recently reported organic moieties based on donor-acceptor systems. The closed aperture measurements confirmed a positive type of nonlinearity, suggesting self-focusing behavior with a magnitude of 2.3×10^{-15} cm^2/W (measured for 100 μM concentration solutions). The transient absorption measurements of donor-acceptor P-$(OH)_2(C_6F_5)_3$-Corrole confirmed a fast excited-state non-radiative relaxation or energy transfer, which can possibly assist in enhancing the nonlinear optical response in these molecules. DFWM measurements confirmed reasonably large $\chi^{(3)}$ values in the range of $6.2–6.9 \times 10^{-14}$ esu (in solution). Time-resolved DFWM depicted an instantaneous response of $\chi^{(3)}$, which confirms the presence of pure electronic nonlinearity. We believe that these synthesized molecules have strong potential for various optoelectronics and photonics applications.

CRediT authorship contribution statement

Naga Krishnakanth Katturi: Investigation, Formal analysis, Writing - original draft, Writing - review & editing. **Shivaprasad Achary Balahoju:** Writing - original draft, Writing - review & editing. **A.R. Ramya:** Investigation, Formal Analysis, Writing - original draft. **Chinmoy Biswas:** Formal analysis, Writing - original draft, Writing - review & editing. **Sai Santosh Kumar Raavi:** Formal analysis, Writing - original draft, Writing - review & editing.**Lingamallu Giribabu:** Supervision, Investigation, Formal Analysis, Writing - original draft, Writing - review & editing. **Venugopal Rao Soma:** Supervision, Formal analysis, Writing - original draft, Writing - review & editing.

Acknowledgments

We thank the DRDO, India, for financial support through the project # ERIP/ER/1501138/M/01/319/D(R&D) dated 27.02.2017. RSSK acknowledges the financial support for the following project numbers BRICS/PilotCall2/IEEE-OSC/2018 (G) and SPARC/2018-2019/P301/SL. LG and AR acknowledged the financial support from the CSIR through MLP-0051 and SRA scheme. We thank Director CSIR-IICT for the support (IICT/Pubs./2019/434).

Declaration of competing interest

The authors declare that they have no known competing financial interests or personal relationships that could have appeared to influence the work reported in this paper.

References

[1] F. Castet, V. Rodriguez, J.-L. Pozzo, L. Ducasse, A. Plaquet, B. Champagne, Design and characterization of molecular nonlinear optical switches, Acc. Chem. Res. 46 (11) (2013) 2656–2665.
[2] A.B. Alemayehu, N.U. Day, T. Mani, A.B. Rudine, K.E. Thomas, O.A. Gederaas, et al., Gold Tris(carboxyphenyl)corroles as multifunctional materials: room temperature near-IR phosphorescence and applications to photodynamic therapy and dye-sensitized solar cells, ACS Appl. Mater. Interfaces 8 (29) (2016) 18935–18942.
[3] I. Aviv, Z. Gross, Corrole-based applications, Chem. Commun. (20) (2007) 1987.
[4] F. D'Souza, O. Ito, Photosensitized electron transfer processes of nanocarbons applicable to solar cells, Chem. Soc. Rev. 41 (1) (2012) 86–96.
[5] R. Mishra, B. Basumatary, R. Singhal, G.D. Sharma, J. Sankar, Corrole-BODIPY dyad as small-molecule donor for bulk heterojunction solar cells, ACS Appl. Mater. Interfaces 10 (37) (2018) 31462–31471.
[6] J. Lu, S. Liu, M. Wang, Push-pull zinc Porphyrins as light-harvesters for efficient dye-sensitized solar cells, Frontiers in Chemistry 6 (2018).
[7] G. Reddy, R. Katakam, K. Devulapally, L.A. Jones, E. Della Gaspera, H.M. Upadhyaya, et al., Ambient stable, hydrophobic, electrically conductive porphyrin hole-extracting materials for printable perovskite solar cells, J. Mater. Chem. C 7 (16) (2019) 4702–4708.
[8] Raavi SSK, C. Biswas, Femtosecond Pump-Probe Spectroscopy for Organic Photovoltaic Devices. Digital Encyclopedia of Applied Physics, Wiley-VCH Verlag GmbH & Co. KGaA, 2019 1–49.
[9] A. Mahammed, K. Chen, J. Vestfrid, J. Zhao, Z. Gross, Phosphorus corrole complexes: from property tuning to applications in photocatalysis and triplet–triplet annihilation upconversion, Chem. Sci. 10 (29) (2019) 7091–7103.
[10] C.B. Kc, G.N. Lim, V.N. Nesterov, P.A. Karr, F. D'Souza, Phenothiazine-BODIPY-fullerene triads as photosynthetic reaction center models: substitution and solvent polarity effects on photoinduced charge separation and recombination, Chemistry 20 (51) (2014) 17100–17112.
[11] D. González-Rodríguez, G. Bottari, Phthalocyanines, subphthalocyanines and porphyrins for energy and electron transfer applications, J. Porphyrins Phthalocyanines 13 (04n05) (2009) 624–636.
[12] D. Gust, T.A. Moore, A.L. Moore, Mimicking photosynthetic solar energy transduction, Acc. Chem. Res. 34 (1) (2001) 40–48.
[13] S.V. Rao, N.K.M.N. Srinivas, D.N. Rao, L. Giribabu, B.G. Maiya, R. Philip, et al., Studies of third-order optical nonlinearity and nonlinear absorption in tetra tolyl porphyrins using degenerate four wave mixing and Z-scan, Opt. Commun. 182 (1–3) (2000) 255–264.
[14] T. Jadhav, R. Maragani, R. Misra, V. Sreeramulu, D.N. Rao, S.M. Mobin, Design and synthesis of donor–acceptor pyrazabole derivatives for multiphoton absorption, Dalton Trans. 42 (13) (2013) 4340.
[15] A. Wojciechowski, M.M.M. Raposo, M.C.R. Castro, W. Kuznik, I. Fuks-Janczarek, M. Pokladko-Kowar, et al., Nonlinear optoelectronic materials formed by push–pull (bi)thiophene derivatives functionalized with di(tri)cyanovinyl acceptor groups, J. Mater. Sci. Mater. Electron. 25 (4) (2014) 1745–1750.
[16] A. Rebane, M. Drobizhev, N.S. Makarov, B. Koszarna, M. Tasior, D.T. Gryko, Two-photon absorption properties of meso-substituted A3-corroles, Chem. Phys. Lett. 462 (4–6) (2008) 246–250.
[17] A. Garai, S. Kumar, W. Sinha, C.S. Purohit, R. Das, S. Kar, A comparative study of optical nonlinearities of trans-A2B-corroles in solution and in aggregated state, RSC Adv. 5 (36) (2015) 28643–28651.
[18] S. Hamad, S.P. Tewari, L. Giribabu, S.V. Rao, Picosecond and femtosecond optical nonlinearities of novel corroles, J. Porphyrins Phthalocyanines 16 (1) (2012) 140–148.
[19] L. Wen, Y. Fang, J. Yang, Y. Han, Y. Song, Third-order nonlinear optical properties and ultrafast excited-state dynamics of benzothiazolium salts: transition in absorption and refraction under different time regimes, Dyes Pigments 156 (2018) 26–32.
[20] L. Wen, Y. Fang, J. Yang, Y. Han, Y. Song, Comparison of third-order nonlinear optical properties of benzothiazolium salt and neutral benzothiazole derivative: broadband absorption response and transient dynamic analysis, Dyes Pigments 168 (2019) 28–35.
[21] Xie Q, Shao Z, Zhao Y, Yang L, Wu Q, Xu W, et al. Novel photo-controllable third-order nonlinear optical (NLO) switches based on azobenzene derivatives. Dyes Pigments. 2019; 170:107599.
[22] W. Xu, W. Wang, J. Li, Q. Wu, Y. Zhao, H. Hou, et al., Two-photon absorption property and excellent optical limiting response of three Schiff base derivatives with large conjugated system, Dyes Pigments 160 (2019) 1–8.
[23] G. Zhai, X. Wu, P. Jin, T. Song, J. Xiao, Y. Song, Synthesis, optoelectronic properties and third-order nonlinear optical behaviors of the functionalized acene derivatives, Dyes Pigments 155 (2018) 93–99.
[24] Yang Y, Wu X, Jia J, Shen L, Zhou W, Yang J, et al. Investigation of ultrafast optical nonlinearities in novel bis-chalcone derivatives. Opt. Laser Technol.. 2020;123: 105903.
[25] L. Giribabu, J. Kandhadi, R.K. Kanaparthi, Phosphorus(V)corrole- Porphyrin based hetero trimers: synthesis, spectroscopy and photochemistry, J. Fluoresc. 24 (2) (2013) 569–577.
[26] J. Kandhadi, V. Yeduru, P.R. Bangal, L. Giribabu, Corrole-ferrocene and corrole-anthraquinone dyads: synthesis, spectroscopy and photochemistry, Phys. Chem. Chem. Phys. 17 (40) (2015) 26607–26620.
[27] T.H. Ngo, D. Zieba, W.A. Webre, G.N. Lim, P.A. Karr, S. Kord, et al., Engaging copper (III) corrole as an electron acceptor: photoinduced charge separation in zinc porphyrin-copper corrole donor-acceptor conjugates, Chemistry 22 (4) (2016) 1301–1312.
[28] M. Tasior, D.T. Gryko, J. Shen, K.M. Kadish, T. Becherer, H. Langhals, et al., Energy- and Electron-transfer processes in Corrole—Perylenebisimide—Triphenylamine Array, J. Phys. Chem. C 112 (49) (2008) 19699–19709.
[29] T. Ding, E.A. Alemán, D.A. Modarelli, C.J. Ziegler, Photophysical properties of a series of Free-Base Corroles, J. Phys. Chem. A 109 (33) (2005) 7411–7417.
[30] F. D'Souza, R. Chitta, K. Ohkubo, M. Tasior, N.K. Subbaiyan, M.E. Zandler, et al., Corrole—fullerene dyads: formation of long-lived charge-separated states in non-polar solvents, J. Am. Chem. Soc. 130 (43) (2008) 14263–14272.
[31] R.D. Teo, J.Y. Hwang, J. Termini, Z. Gross, H.B. Gray, Fighting Cancer with Corroles, Chem. Rev. 117 (4) (2016) 2711–2729.
[32] I. Aviv-Harel, Z. Gross, Aura of Corroles, Chem. Eur. J. 15 (34) (2009) 8382–8394.
[33] H.L. Buckley, W.A. Chomitz, B. Koszarna, M. Tasior, D.T. Gryko, P.J. Brothers, et al., Synthesis of lithium corrole and its use as a reagent for the preparation of cyclopentadienyl zirconium and titanium corrole complexes, Chem. Commun. 48 (87) (2012), 10766. .

[34] H. Agadjanian, J. Ma, A. Rentsendorj, V. Valluripalli, J.Y. Hwang, A. Mahammed, et al., Tumor detection and elimination by a targeted gallium corrole, Proc. Natl. Acad. Sci. 106 (15) (2009) 6105–6110.
[35] R. Capuano, G. Pomarico, R. Paolesse, C. Di Natale, Corroles-porphyrins: a teamwork for gas sensor arrays, Sensors (Basel) 15 (4) (2015) 8121–8130.
[36] S.M. Borisov, A. Alemayehu, A. Ghosh, Osmium-nitrido corroles as NIR indicators for oxygen sensors and triplet sensitizers for organic upconversion and singlet oxygen generation, J. Mater. Chem. C 4 (24) (2016) 5822–5828.
[37] J. Barber, P.D. Tran, From natural to artificial photosynthesis, J. R. Soc. Interface 10 (81) (2013), 20120984. .
[38] T.S. Balaban, Tailoring porphyrins and chlorins for self-assembly in biomimetic artificial antenna systems, Acc. Chem. Res. 38 (8) (2005) 612–623.
[39] S. Nardis, F. Mandoj, M. Stefanelli, R. Paolesse, Metal complexes of corrole, Coord. Chem. Rev. 388 (2019) 360–405.
[40] A. Mahammed, Z. Gross, Corroles as triplet photosensitizers, Coord. Chem. Rev. 379 (2019) 121–132.
[41] T. Stensitzki, Y. Yang, A. Berg, A. Mahammed, Z. Gross, K. Heyne, Ultrafast electronic and vibrational dynamics in brominated aluminum corroles: energy relaxation and triplet formation, Structural Dynamics 3 (4) (2016), 043210. .
[42] E. Pomarico, P. Pospisil, M.E. Bouduban, J. Vestfrid, Z. Gross, S. Záliš, et al., Photophysical heavy-atom effect in iodinated metallocorroles: spin–orbit coupling and density of states, J. Phys. Chem. A 122 (37) (2018) 7256–7266.
[43] Y. Yang, D. Jones, T. von Haimberger, M. Linke, L. Wagnert, A. Berg, et al., Assignment of aluminum corroles absorption bands to electronic transitions by femtosecond polarization resolved Vis-pump IR-probe spectroscopy, J. Phys. Chem. A 116 (3) (2012) 1023–1029.
[44] X. Liu, A. Mahammed, U. Tripathy, Z. Gross, R.P. Steer, Photophysics of Soret-excited tetrapyrroles in solution. III. porphyrin analogues: aluminum and gallium corroles, Chem. Phys. Lett. 459 (1–6) (2008) 113–118.
[45] S.S. Raavi, J. Yin, G. Grancini, C. Soci, S.V. Rao, G. Lanzani, et al., Femtosecond to microsecond dynamics of soret-band excited corroles, J. Phys. Chem. C 119 (52) (2015) 28691–28700.
[46] P. Yadav, T. Anand, S.S.B. Moram, S. Bhattacharya, M. Sankar, S.V. Rao, Synthesis and femtosecond third order nonlinear optical properties of push-pull trans- a 2 B-corroles, Dyes Pigments 143 (2017) 324–330.
[47] X. Liang, J. Mack, L.M. Zheng, Z. Shen, N. Kobayashi, Phosphorus(V)-corrole: synthesis, spectroscopic properties, theoretical calculations, and potential utility for in vivo applications in living cells, Inorg. Chem. 53 (6) (2014) 2797–2802.
[48] A. Ghosh, M. Ravikanth, Synthesis, structure, spectroscopic, and electrochemical properties of highly fluorescent phosphorus (V)–meso-triarylcorroles, Chem Eur J 18 (20) (2012) 6386–6396.
[49] S. Bhattacharya, C. Biswas, S.S.K. Raavi, J. Venkata Suman Krishna, N. Vamsi Krishna, L. Giribabu, et al., Synthesis, optical, electrochemical, DFT studies, NLO properties, and ultrafast excited state dynamics of carbazole-induced phthalocyanine derivatives, J. Phys. Chem. C 123 (17) (2019) 11118–11133.
[50] J.J. Snellenburg, S.P. Laptenok, R. Seger, K.M. Mullen, I.H.M.V. Stokkum, Glotaran: AJava-based graphical user Interface for theRPackageTIMP, J. Stat. Softw. 49 (3) (2012).
[51] M. Gouterman, Spectra of porphyrins, J. Mol. Spectrosc. 6 (1961) 138–163.
[52] I.H. van Stokkum, D.S. Larsen, R. van Grondelle, Global and target analysis of time-resolved spectra, Biochimica et Biophysica Acta (BBA)-Bioenergetics 1657 (2–3) (2004) 82–104.
[53] K.N. Krishnakanth, S. Seth, A. Samanta, S. Venugopal Rao, Broadband ultrafast nonlinear optical studies revealing exciting multi-photon absorption coefficients in phase pure zero-dimensional Cs_4PbBr_6 perovskite films, Nanoscale 11 (3) (2019) 945–954.
[54] B.S. Achary, A.R. Ramya, J.B. Nanubolu, S. Seetharaman, G.N. Lim, Y. Jang, et al., Axially substituted phosphorous(v) corrole with polycyclic aromatic hydrocarbons: syntheses, X-ray structures, and photoinduced energy and electron transfer studies, New J. Chem. 42 (10) (2018) 8230–8240.
[55] K. Fujino, Y. Hirata, Y. Kawabe, T. Morimoto, A. Srinivasan, M. Toganoh, et al., Confusion and neo-confusion: Corrole isomers with an NNNC Core, Angew. Chem. Int. Ed. 50 (30) (2011) 6855–6859.
[56] P.T. Anusha, D. Swain, S. Hamad, L. Giribabu, T.S. Prashant, S.P. Tewari, et al., Ultrafast excited-state dynamics and dispersion studies of third-order optical nonlinearities in novel corroles, J. Phys. Chem. C 116 (33) (2012) 17828–17837.
[57] D. Swain, V.K. Singh, N.V. Krishna, L. Giribabu, S.V. Rao, Optical, electrochemical, third-order nonlinear optical, and excited state dynamics studies of thio-zinc phthalocyanine, J. Porphyrins Phthalocyanines 18 (4) (2014) 305–315.
[58] J.L. Humphrey, D. Kuciauskas, Charge transfer enhances two-photon absorption in transition metal porphyrins, J. Am. Chem. Soc. 128 (12) (2006) 3902–3903.
[59] R.S.S. Kumar, S.V. Rao, L. Giribabu, D.N. Rao, Ultrafast nonlinear optical properties of alkyl phthalocyanines investigated using degenerate four-wave mixing technique, Opt. Mater. 31 (6) (2009) 1042–1047.
[60] S. Bhattacharya, C. Biswas, S.S.K. Raavi, J.V.S. Krishna, D. Koteshwar, G. Lingamallu, V.R. Soma, Synthesis, Optical, Electrochemical, DFT Studies, NLO Properties and Excited State Dynamics of a Triphenyl Imidazole Induced Phthalocyanine Derivative, RSC Adv. 9 (63) (2019) 36726.